ResearchGate

See discussions, stats, and author profiles for this publication at: https://www.researchgate.net/publication/253061358

The wetting characteristics and diffusive growth of precursing films in single and multicomponent metallic systems

ARTICLE · JANUARY 2003

READS
20

1 AUTHOR:

Jaehyun Moon
Electronics and Telecommunications Resear…

82 PUBLICATIONS **666** CITATIONS

SEE PROFILE

Available from: Jaehyun Moon
Retrieved on: 01 February 2016

Pseudopartial Wetting and Precursor Film Growth in Immiscible Metal Systems

Jaehyun Moon,[†] Stephen Garoff,*[,‡,§] Paul Wynblatt,[†] and Robert Suter[‡]

Department of Materials Science and Engineering, Department of Physics, and Center for Complex Fluids Engineering, Carnegie Mellon University, Pittsburgh, Pennsylvania 15213

Received August 5, 2003. In Final Form: November 3, 2003

We explore the equilibrium wetting behavior and precursor film growth in pure and alloy metallic systems. The systems exhibit equilibrium "pseudopartial" wetting, that is, a thin film in equilibrium with a nonzero contact angle in both liquid and solid states. The film spreading kinetics clearly indicates a diffusive transport mechanism. The alloying has only a small impact on the equilibrium wetting properties but strongly affects the transport during the growth of the precursor film.

1. Introduction

We address two fundamental questions in wetting. Are there circumstances under which a thin film coexists in equilibrium with a macroscopic body having a nonzero contact angle? What is the mass transport mechanism during the growth of such films? Theoretical models have predicted conditions under which such "pseudopartial" wetting, that is, a thin film in equilibrium with a nonzero contact angle, will take place.[1−3] While many partial wetting systems with nonzero contact angles and no films have been studied, experimental examples of pseudopartial wetting have not been explicitly recognized in the literature. Whereas ∼10-μm-long surfactant self-assembled monolayers (SAMs) attached to contact lines of surfactant solutions having finite contact angles have been observed, [4−7] these systems are not in equilibrium as demonstrated by marked differences in behavior at advancing and receding contact lines. Although not recognized as representing pseudopartial wetting, several instances have been observed in metal-on-metal systems.[8−10]

The existence of thin films attached to contact lines was discovered in 1919 by Hardy[11] and also by Bascom et al.[12] and Heslot et al.[13] The thin films have recently been studied by optical ellipsometry[14,15] and molecular dynamics simulations.[16,17] These studies address the growth of precursor films in polymeric liquids that are spreading toward a 0° contact angle. They find that the motion of an isoconcentration point in the film moves with a $\sqrt{t}$ dependence for both oligomeric and polymeric polydimethylsiloxane.

Here, we examine the phenomena of pseudopartial wetting and precursor film growth of metallic systems in an ultrahigh vacuum (UHV) environment. The UHV apparatus affords us both a clean environment and electron-beam-based diagnostic tools. The cleanliness of the UHV environment allows us to study wetting phenomena without the complexities of contact angle hysteresis and solutal Maragoni stresses that likely occur because of contamination in an ambient environment. As a result of the exceedingly low vapor pressure of our systems, evaporation is negligible, simplifying both the film[18] and contact angle[19] behaviors. In our alloy system, the low vapor pressures also remove the possibility of differential evaporation of various components, which can cause instabilities in contact lines[20] or dominate transport in precursor films.[12] The electron-based diagnostic tools allow the measurement of composition and density within the precursor film at submicrometer resolution. Thus, we can characterize the film growth by tracking the full compositional profile as it evolves with time. Finally, the nonzero contact angle of the systems investigated here ensures that the advancing contact line of a spreading drop is not influencing the film growth.

The three systems we have studied, pure Pb, pure Bi, and a Pb−Bi alloy, on the Cu(111) surface, exhibit pseudopartial wetting. We have measured the Pb/Cu(111) system in both solid and liquid Pb states and find pseudopartial wetting in both cases. We have followed the dynamics of thin film growth in all three systems and found all aspects of the transport to be compatible with

* Author to whom correspondence should be addressed.
[†] Department of Materials Science and Engineering, Carnegie Mellon University.
[‡] Department of Physics, Carnegie Mellon University.
[§] Center for Complex Fluids Engineering, Carnegie Mellon University.

(1) Brochard-Wyart, F.; di Meglio, J.-M.; Quéré, D.; de Gennes, P. *Langmuir* **1991**, *7*, 335.
(2) Sharma, A.; *Langmuir* **1993**, *9*, 3580.
(3) Hirasaki, G. Shapes of meniscus and film transition region. In *Interfacial phenomena in petroleum recovery*; Morrow, N., Ed.; Marcel Dekker: New York, 1991.
(4) Decker, E. L.; Frank, B.; Suo, Y.; Garoff, S. *Colloids Surf., A* **1999**, *156*, 177.
(5) Frank, B.; Garoff, S. *Colloids Surf., A* **1996**, *116*, 31.
(6) Qu, D.; Suter, R.; Garoff, S. *Langmuir* **2002**, *18*, 1649.
(7) Kumar, N.; Varanasi, K.; Tilton, R.; Garoff, S. *Langmuir* **2003**, *19*, 5366.
(8) Rao, G.; Zhang, D.; Wynblatt, P. *Acta Metall. Mater.* **1993**, *11*, 3331.
(9) Shi, Z.; Wynblatt, P. *Metall. Mater. Trans. A* **2002**, *33*, 1003.
(10) Moon, J.; Lowekamp, J.; Wynblatt, P.; Garoff, S.; Suter, R. *Surf. Sci.* **2001**, *488*, 73.
(11) Hardy, W. *Philos. Mag.* **1919**, *49*, 38.
(12) Bascom, W.; Cottington, R.; Singleterry, C. Dynamic surface phenomena in the spontaneous spreading of oils on solids. In *Contact Angle, Wettability, and Adhesion*; Gould, R.; Ed.; Advances in Chemistry Series 43; American Chemical Society: Washington, DC, 1964.
(13) Heslot, F.; Cazabat, A.-M.; Levinson, P.; Fraysse, N. *Phys. Rev. Lett.* **1990**, *65*, 599.
(14) Voué, M.; Valignat, M.; Oshanin, G.; Cazabat, A.-M. *Langmuir* **1999**, *15*, 1522.
(15) Fraysse, N.; Valignat, M.; Cazabat, A.-M.; Heslot, F.; Levinson, P. *J. Colloid Interface Sci.* **1993**, *158*, 27.
(16) De Coninck, J.; Fraysse, N.; Valignat, M.; Cazabat, A.-M. *Langmuir* **1993**, *9*, 1906.
(17) Voué, M.; De Coninck, J. *Acta Mater.* **2000**, *48*, 4405.
(18) Wayner, P., Jr. *J. Colloid Interface Sci.* **1980**, *77*, 495.
(19) Davis, S. *J. Appl. Mech.* **1983**, *50*, 977.
(20) Fournier, J.; Cazabat, A.-M. *Europhys. Lett.* **1992**, *20*, 517.

10.1021/la030323j CCC: $27.50 © 2004 American Chemical Society
Published on Web 12/19/2003

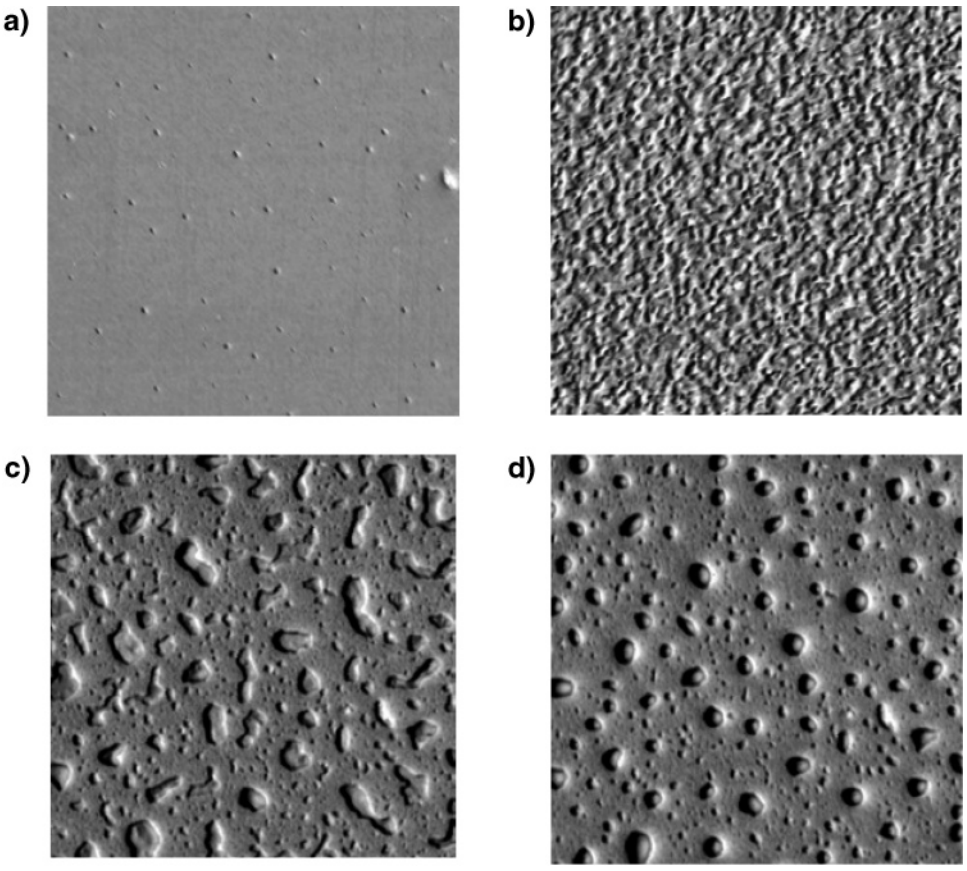

Figure 1. Dewetting sequence of a Pb−Bi alloy film: (a) initial film, (b) initiation of film breakup, (c) just after partial dewetting, and (d) 1 min after dewetting. (Size of each photo is 100 μm × 100 μm.)

diffusion. We observe significant concentration variations across the moving films, and we see the influence of adsorbate/surface interactions peculiar to individual systems. In the alloy system, the relative Bi/Pb concentrations are seen to be different (i) in the bulk phase, (ii) on the surface of the bulk phase, (iii) in the equilibrium thin film, and (iv) at the growing tip of the thin film. These concentration variations have only a slight effect on the equilibrium wetting behavior but a dramatic effect on the dynamics.

Our measurements cover a temperature range (353−623 K) over which both the bulk phases and the thin films of Pb go from solid (or ordered) to liquid (or disordered). The static wetting behaviors and even the dynamics are qualitatively independent of these phase transitions. We believe that this observation makes our work on metallic systems relevant to those interested in the behavior of even complex and polymeric systems near room temperature.

2. Experiments

2.1. Apparatus. Samples were prepared by physical vapor deposition (PVD) in a UHV chamber with a base pressure of 10^{-10} Torr. This chamber is equipped with an evaporator for performing depositions, an Auger electron spectrometer for surface composition analysis, and an Ar ion sputtering gun for surface cleaning.

Wetting studies were carried out in a scanning Auger microprobe (SAM) system. Spatially resolved Auger electron spectroscopy (AES) measurements have a resolution of 0.1 μm. In addition, imaging based on secondary electron emission, as in a scanning electron microscope, can be carried out with 0.1-μm resolution.

2.2. Sample Preparation and the Dewetting Process. One-micrometer-thick films of Pb, Bi, and Pb−11 atom % Bi (hereafter Pb−Bi alloy) were deposited on Cu(111) surfaces in the PVD system. Prior to deposition, the (111) oriented Cu single crystals were cleaned by several cycles of annealing followed by Ar ion sputtering. This procedure depletes the near-surface region of impurities that might otherwise segregate to the surface during subsequent heating. The Pb and Pb−Bi alloy films covered the entire Cu surface. For the Bi sample, a Ta foil masked half the Cu surface, producing a sharp demarcation line between the film and the bare surface. The micrometer-thick film samples were transferred to the SAM. The surface was then lightly sputtered to remove any contamination that might have been acquired during transfer, and Auger spectra were used to verify a clean surface.

Next, Pb and Pb−Bi alloy films were gradually heated to a temperature just above the melting point of the film material. Upon melting, the film dewetted from the Cu surface to produce isolated metal drops of sizes ranging from 5 to 20 μm. Upon subsequent cooling, the drops solidified into small single crystals. A sequence of images acquired during the dewetting process of the alloy sample is shown in Figure 1. It should be noted that the Pb−Bi thick film melts over a range of temperatures from 538 to 568 K, making it possible to observe the process. Solidified drops of pure Pb are shown in Figure 2. That the solidified drops are single crystals can be seen by the presence of the (111) facets lying parallel to the substrate surface.[8] Such facets are well-known to be present on the equilibrium crystal shape of pure Pb.[21] No analogous dewetting procedure was used on the Bi sample. Thus, the spreading experiments described in the following were done in a two-dimensional geometry for the Pb and Pb−Bi alloy samples and a one-dimensional geometry for the Bi sample. The appropriate analysis is described below.

Carbon and oxygen were the only surface impurities detected at the various surfaces by AES. The presence of these impurities was carefully monitored during all the experiments. Any traces were removed by sputtering. Unless otherwise noted, all experimental results were performed on clean surfaces with

(21) Metois, J.; Heyraud, J. *J. Cryst. Growth* **1982**, *57*, 487.

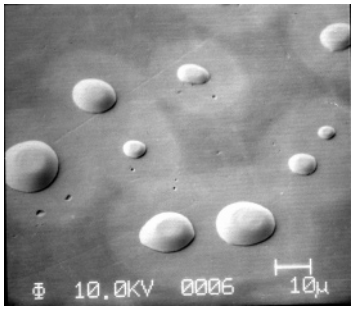

Figure 2. Pb particles and Pb "halos" around the Pb drops on the Cu substrate.

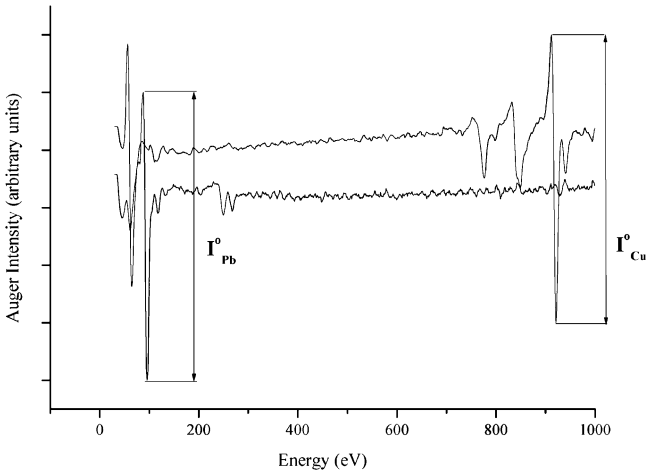

Figure 3. Standard Auger spectra: Pb (92 eV) and Cu (920 eV).

impurity concentrations within the experimental noise. Figure 3 shows differentiated Auger spectra obtained from clean Pb crystallites and the Cu(111) substrate.

2.3. Data Acquisition. We used two types of measurements to detect spreading kinetics. First, Auger line scans were analyzed to yield detailed information about component compositions as a function of position. The Auger transitions of Pb at 89 eV (a doublet), of Bi at 104 eV (a doublet), and of Cu at 920 eV (a singlet) were used to quantify the surface concentrations. For the alloy sample, to minimize the effects of Auger peak overlap, we used only the lower energy transition of Pb and the higher energy transition of Bi. Quantification of surface coverage was accomplished by the scheme of Seah,[22] from which the coverage [Γ_X, expressed in monolayers (MLs)] of a given element X in the precursor film, is related to the intensity ratio of the Auger peaks in pure reference standards (I_X^0/I_{Cu}^0) and that obtained from a sample of interest (I_X/I_{Cu}). For the present purposes, we define a coverage of one monolayer as 9.4×10^{14} atoms/cm^2. This is the number of Pb atoms per unit area in the bulk (111) plane of pure Pb. For comparison, the Cu(111) surface has 3.9×10^{15} atoms/cm^2.

The second method of following spreading is illustrated in Figure 4. We found it possible to use scanning electron microscopy (SEM) measurements to image the extent of thin film progression over a broad area of the surface. The films are the halos surrounding the Pb drops in Figure 4. By comparing a SEM image and an Auger line scan in the same region, we determined that the detectable edge of the SEM halo occurs at ~0.8 ML of Pb. While SEM photos allow determination only of the extent of a fixed threshold coverage, they are essential for observing the kinetics of disordered films that spread too quickly for complete Auger analysis. In a one-dimensional geometry, a diffusion coefficient can be extracted by tracking this isoconcentration point using $x = (Dt)^{1/2}$. As discussed in the following, spreading from drops requires a more sophisticated analysis.

(22) Seah, M. Quantification of AES and XPS. In *Practical surface analysis by Auger and X-ray photoelectron spectroscopy*; Briggs, D. M., Seah, M., Eds.; Academic Press: New York, 1969.

We prepared samples for dynamics measurements as follows. Dewetted samples were heated to a preselected temperature, were held at that temperature to allow drops and films to reach thermal equilibrium, and then were sputtered to remove the film. We carefully allow sufficient annealing time to ensure that the droplets have reached equilibrium even in the solid state. The end of the sputtering establishes the time $t = 0$ for the spreading measurement. The spreading of the films was measured for periods from 15 min to 10 h. A similar procedure was used for the pure Bi case: the sample was raised to the selected temperature, then any film was sputtered away and subsequent film growth away from the linear film/substrate interface was measured.

2.4. Temperature and Phases. As mentioned in the Introduction, we have measured spreading from both liquid and solid macroscopic bodies connected to both ordered and disordered films. The bulk melting point is easy to identify from the abrupt disappearance of the facets at the tops of the solid drops, and we use this as a calibration of our temperature measurement. We use the film's diffusivity (see section 3.2 for details) to determine its own order−disorder temperature. Figure 5 shows the Arrhenius plot for the diffusion constants of Pb over Cu(111) obtained at a coverage of 0.8 ML. Film melting is indicated by the change in the slope of the plot, which indicates a change in the activation energy for diffusion. This break in the slope occurs near 590 K, which is lower than the bulk melting temperature of Pb (600 K) and is in agreement with a low-energy electron diffraction study for the disordering of a Pb monolayer film on Cu(111).[23] Thus, the data point at 590 K corresponds to a disordered film spreading from a bulk solid drop. High temperatures have both the bulk and the film in disordered phases.

3. Results and Discussion

3.1. Equilibrium Contact Angles and Film Compositions. The dewetting process yields virtually the same film coverage and macroscopic contact angle as that which we observe when films regrow out of the droplets. The receding contact lines of the liquid Pb drops during dewetting leave behind films ~0.82 ML in thickness. This coverage is essentially the same as that of the films produced by film regrowth from the drops, ~0.85 ML (see section 3.2 for details). The small difference may be attributed to the presence of impurities (mainly C) at the surface when the film initially undergoes dewetting. If anything, the presence of impurities is likely to selectively attenuate the (lower energy) Pb Auger signal in relation to the (higher energy) Cu Auger signal, thus leading to estimates of Pb coverage for the dewetted films, which might be too low. In all cases, contact angles found on dewetting and after film regrowth were within the experimental uncertainty. Thus, we conclude that the film covered surface coexisting with macroscopic bodies (either droplets or a half-covered surface) with finite contact angles are equilibrium structures rather than transient dynamic states or even static but metastable structures.

Macroscopic contact angles, as measured from SEM photos after full equilibration at preselected temperatures, are shown in Figure 6. Because there are no facets on the solid drops along the contact line, no ambiguity occurs in the contact angle measurements. The vertical axis, cos θ, represents the energy ratio, $(\gamma_{S/V} - \gamma_{S/drop})/\gamma_{drop/V}$, according to Young's equation. The indicated melting temperatures refer to bulk melting for pure Pb and to the liquidus temperature for the case of the Pb−Bi alloy. We emphasize that the surface energies (γ's) are not those of the bare interfaces but represent adsorption-modified values. As can be seen from Figure 6 for each type of sample, the cos θ values are only mildly sensitive to either the temperature or the physical state of the drop and film.

(23) Meyer, G.; Michailov, M.; Henzler, M. *Surf. Sci.* **1988**, *202*, 125.

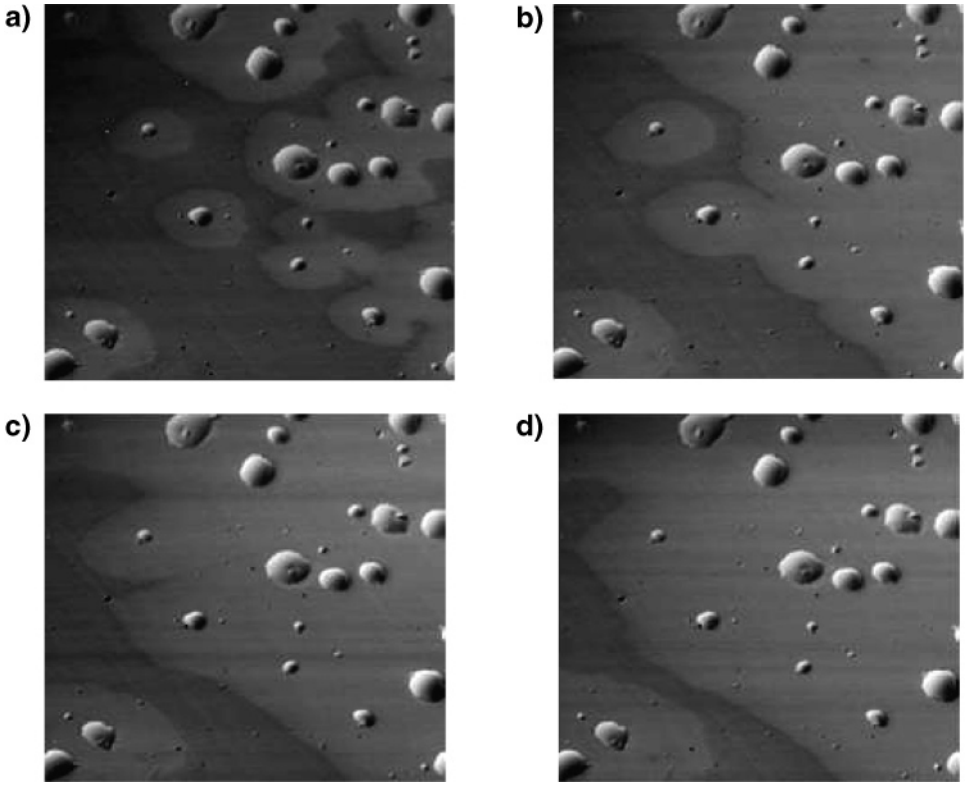

Figure 4. Pb precursor wetting film evolution on Cu(111) at 603 K (size of each photo is 150 μm × 140 μm): (a) 3, (b) 8, (c) 13, and (d) 20 min.

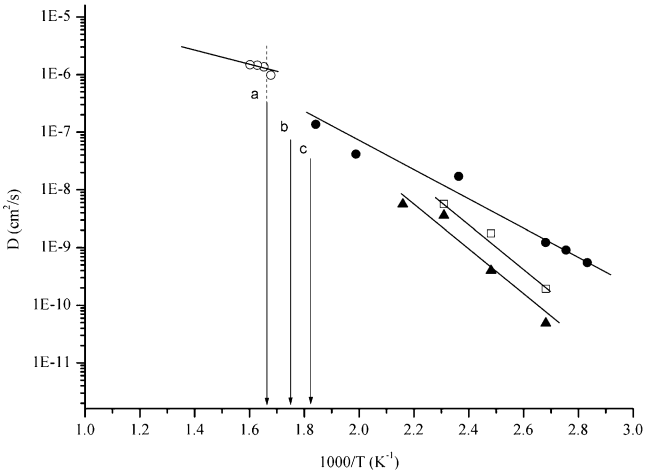

Figure 5. Arrhenius plot of monolayer growing from (●) solid Pb; (○) liquid Pb; (□) solid Bi; and (▲) the solid Pb−Bi alloy. Bulk melting points of (a) pure Pb, (b) Pb−Bi, and (c) pure Bi.

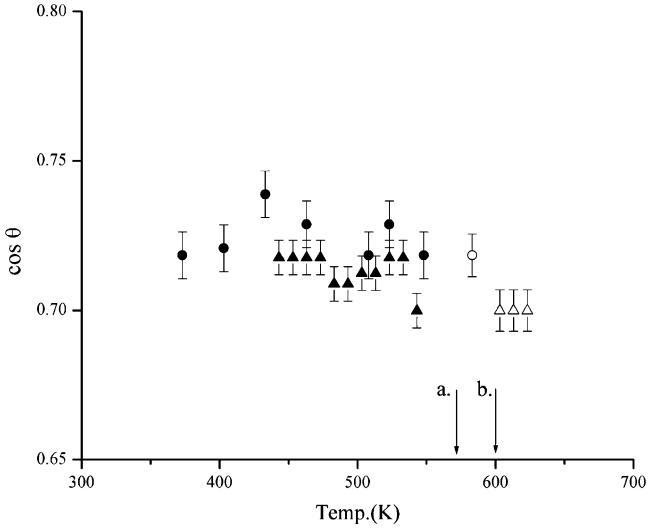

Figure 6. Macroscopic contact angles of Pb and Pb−Bi drops on Cu(111): (▲) pure Pb solid, (△) pure Pb liquid, (●) Pb−Bi alloy solid, and (○) Pb−Bi alloy liquid. Bulk melting points of (a) Pb−Bi alloy (liquidus) and (b) pure Pb.

Thus, all three systems investigated here exhibit "pseudopartial wetting", that is, a film in equilibrium with a nonzero contact angle.[8,10] This is distinct from partial wetting where there is no film attached to a nonzero contact angle. Despite considerable speculation about the existence of pseudopartial wetting,[1−3] experimental evidence of its existence has been indirect. The results presented here represent some of the first direct measurements of the presence of a film and its structure in equilibrium with a nonzero contact angle.

Pb−Bi alloys offer a convenient model system for exploring the effects of the presence of two components on the composition and spreading kinetics of precursor films. At the temperatures studied here, the limit of solubility of Bi in Pb is ∼20 atom %, so the Pb−Bi bulk alloy exists as a solid solution. In general, one expects the surface of a binary alloy to be enriched either in solute or in solvent. Several factors can be at play in adsorption at solid surfaces; however, the dominant factor in this case is most likely related to the fact that the surface energy of Bi is lower than that of Pb (γ_{Bi} = 505 mJ/m^2 and γ_{Pb} = 560 mJ/m^2). Auger analysis of the Pb−Bi drops yielded drop surface compositions of 22 and 24 atom % Bi at temperatures of 373 and 463 K, respectively. This rather weak segregation of Bi to the surfaces of dilute Pb−Bi alloys, to produce a surface enrichment by about a factor of 2, is consistent with previous observations.[24]

In the case of the precursor film of the alloy, its equilibrium composition will also be driven by adsorption

(24) Wang, Z.; Wynblatt, P.; Chatain, D. *Interface Sci.* **1999**, *7*, 173.

considerations. The surface energy of Cu is $\gamma_{Cu} = 1520$ mJ/m^2. Thus, there is a strong driving force for adsorption of both Bi and Pb at the Cu surface, with a slight advantage for Bi adsorption. However, the equilibrium composition of the film should be related to the surface segregation behavior of a ternary Cu−Bi−Pb alloy saturated with Pb and Bi. In such a ternary solution, the surface composition depends on interactions among the three components,[25] and the resulting behavior is somewhat more complex than in the binary Pb−Bi alloy. Auger analysis of the film yielded equilibrium Bi concentrations ranging from 71 atom % to 55 atom % Bi in the temperature range from 373 to 463 K.

We note that the equilibrium Bi concentrations at the drop surface and in the precursor film decrease with increasing temperature but with different temperature dependences. This trend is consistent with theories of surface segregation.[26,27] However, it is important to emphasize that the *total* coverage in the equilibrium precursor film on Cu is essentially independent of the Bi concentration in the film. The total coverages of pure Pb, pure Bi, and the Pb−Bi alloy are 0.85, 0.88, and 0.87 ML, respectively. Because the atomic sizes of Pb and Bi are approximately equal but larger than the atomic size of Cu, this maximum coverage is most likely related to atomic size effects.

As shown in Figure 6, the contact angle for the Pb−Bi alloy is not much different from that in the case for the pure materials and also shows a weak temperature dependence. In the case of the Pb−Bi alloy, composition changes in the precursor film will not have a strong effect on the contact angle because the total coverage of Pb + Bi is essentially the same as the coverage in the cases of pure Pb and Bi wetting phases and, hence, the values of $\gamma_{S/V}$ will be the same in all cases. In contrast, the composition changes at the drop surface could play a role in determining the contact angle. However, in view of the weak segregation of Bi to the Pb−Bi surface, only small effects on the surface energy of the drop are expected. Without resorting to elaborate calculations, we conclude that variations in the contact angle in the case of the Pb−Bi wetting phase due to Bi adsorption are most likely concealed within the experimental error of the measurements.

3.2. Spreading Kinetics of Precursor Films. The material transport mechanism in precursor films has been the subject of discussion in the literature.[12,28−32] Precursor films in the Pb, Bi, and Pb−Bi systems studied here all show diffusive growth. In the following we describe our results showing this, while details of the analysis of the diffusion process appear elsewhere.[10,33,34]

3.2.1. Bi on Cu(111). The diffusion of Bi over the Cu(111) substrate is the simplest case to analyze because in this case the sample geometry produces one-dimensional growth (see section 2.2). If the spreading mechanism of a film is diffusional and one-dimensional, then all the isoconcentration points move as $x/t^{1/2}$ even if the diffusion constant, D, is a function of the concentration.[35] Thus, Γ versus $x/t^{1/2}$ should be invariant at a constant temperature for a given material system. Bi coverage profiles in the vicinity of the slablike Bi source, obtained by Auger line scans at 433 K, are plotted in Figure 7 as the normalized coverage, c, versus $x/t^{1/2}$ ($c = \Gamma/\Gamma_0$, where Γ_0 is the equilibrium coverage). As can be seen, all the profiles superimpose when plotted in this space, consistent with a diffusional character of precursor film growth. The rather precipitous decline in coverage beyond the region of near-monolayer coverage indicates that growth is much faster at a high coverage than in the submonolayer films as a result of the variation in D with the concentration. The Arrhenius plot for the Bi film in Figure 5 is again strongly suggestive of a diffusive growth.

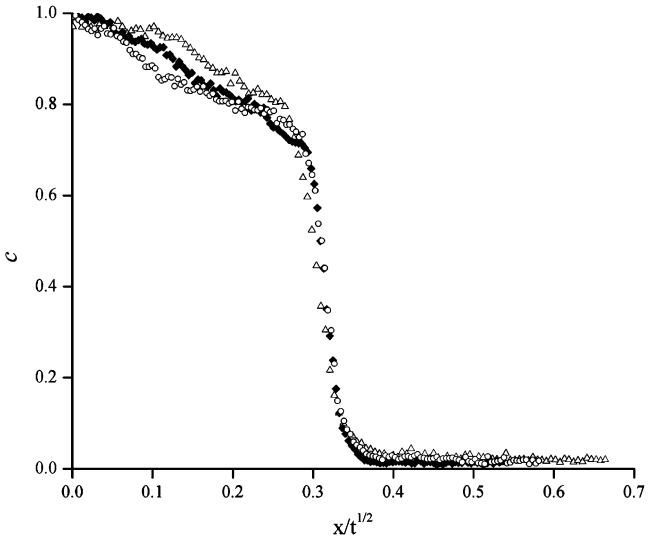

Figure 7. Invariance of Bi spreading on Cu(111) at 433 K: (△) 2 h; (◆) 3 h, 45 min; and (○) 4 h.

3.2.2. Pb on Cu(111). The case of profiles spreading over a two-dimensional substrate from a circular source, such as our Pb and Pb−Bi drops, leads to somewhat more complex solutions of Fick's second law, especially if the diffusivity is a function of the concentration (i.e., coverage). In this case, an isoconcentration point a distance r from the center of the cylindrical source moves as a power series in $t^{n/2}$ ($n = 1, 2, 3, ...$).[35] The two-dimensional character of the film growth from the Pb drop is seen in Figure 8. The y axis is the spreading length, x, of the precursor film away from the edge, normalized by drop radius, r_0. As can been seen, at short annealing times (<90 s$^{1/2}$), $x/r_0 \propto t^{1/2}$ is a reasonable approximation even in cylindrical geometry. The deviation at long annealing times is due to the cylindrical geometry and to the surface-coverage-dependent diffusion coefficients, $D(c)$. We note that the $t^{1/2}$ kinetics observed here are quite similar to those observed in the spreading of polymeric solutions,[31,36,37] despite the latter's many internal degrees of freedom.

Previously, we have reported details of the growth of Pb precursor films, attached to Pb drops on Cu(111)

(25) Serre, C.; Chatain, D.; Wynblatt, P.; Muris, M.; Bienfait, M. *Metall. Mater. Trans. A* **2001**, *32*, 2851.
(26) McLean, D. *Grain Boundaries in Metals*; Oxford Press: London, 1957.
(27) Guttman, M.; McLean, D. In *Interfacial Segregation*; Johnson, W. W., Blackely, J., Eds.; ASM: Metal Parks, OH, 1979.
(28) Cazabat, A.-M.; Valignat, M.; Villette, S.; De Coninck, J.; Louche, F. *Langmuir* **1997**, *13*, 4754.
(29) Ala-Nissila, T.; Herminghaus, S.; Hjelt, T.; Leiderer, P. *Phys. Rev. Lett.* **1996**, *76*, 4003.
(30) Cazabat, A.-M. *Contemp. Phys.* **1987**, *28*, 347.
(31) Burlatsky, S.; Oshanin, G.; Cazabat, A.-M.; Moreau, M.; Reinhardt, W. *Phys. Rev. E* **1996**, *54*, 3832.
(32) Lukkarinen, A.; Kaski, K.; Abraham, D. *Phys. Rev. E* **1995**, *51*, 2199.
(33) Moon, J.; Wynblatt, P.; Garoff, S.; Suter, R. *Surf. Sci.*, in preparation.
(34) Moon, J.; Wynblatt, P.; Garoff, S.; Suter, R. *Acta Mater.*, in preparation.
(35) Philip, J.; Theory of infiltration. In *Advances in Hydroscience*; Chow, V., Ed.; Academic Press: New York, 1969; Vol. 5.
(36) De Coninck, J.; Fraysse, N.; Valignat, M.; Cazabat, A.-M. *Langmuir* **1993**, *9*, 1906.
(37) Voué, M.; Valignat, M.; Oshanin, G.; Cazabat, A.-M. *Langmuir* **1999**, *15*, 1522.

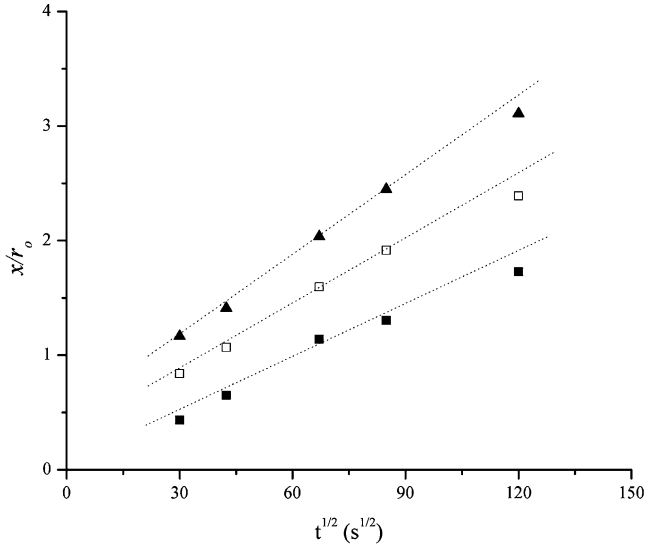

Figure 8. Spreading kinetics of Pb on Cu(111) at various coverages at 373 K. x, diffusion length; r_0, drop radius. (■) 1 ML; (□) 0.5 ML; and (▲) 0.2 ML.

substrates.[10] Here, we summarize important results briefly. Examples of spreading profiles of Pb on Cu(111) obtained at 373 K are shown in Figure 9a. The central parts of the profiles with a high Pb concentration define the location of the Pb drop. The relatively flat shoulders next to the Pb drop represent the Pb coverage in local equilibrium with the drop, which achieves a maximum of 0.85 ML. The maximum coverage was found to be constant over all the annealing times, with no evidence of layering of films. The nonmonotonic changes in the slopes of the profiles reflect the fact that the spreading rate is coverage-dependent. The diffusion coefficients extracted from profiles by means of Fick's second law are found to be high at both low and high Pb coverages and display a minimum at a coverage of about 0.5 ML (see Figure 9b). These changes in the diffusivity have been interpreted from the known sequence of structures of Pb on Cu(111) that develop as a function of the Pb coverage.

3.2.3. Comparison of the Pure Pb and Bi Cases. Pb and Bi films exhibit significantly different growth patterns. It is clear from Figures 5 and 10 that Bi spreads much more slowly than Pb. Of greater interest is the contrast of the concentration profiles. Bi profiles (Figure 7) show a roughly linear gradient across the film and a precipitous drop in coverage corresponding to the end of the film. Pb, on the other hand, has a more complex profile (Figure 9a) with a substantial submonolayer region that displays several inflection points. These profiles reflect the fact that Bi diffusivity decreases from high coverages to the submonolayer region, whereas Pb diffusivity is lowest at midrange coverages.

3.2.4. Pb−Bi Alloy on Cu(111). Figure 11 shows the composition of the alloy film as a function of the distance from the parent drop at two different times. The high Bi/Pb ratio near the contact line is essentially the same as that of the equilibrium film composition, whereas the submonolayer region far from the contact line is enriched in Pb. This is consistent with the fact that, in pure systems, the Pb spreading rate is higher than that of Bi.

Figure 10 compares the spreading profiles of the alloy with those of the pure samples. In all cases, the maximum coverage near the source corresponds to the equilibrium film composition. The equilibrium films retain this coverage and show no evidence of layering. The spreading profile of Bi in the Pb−Bi film qualitatively resembles that of

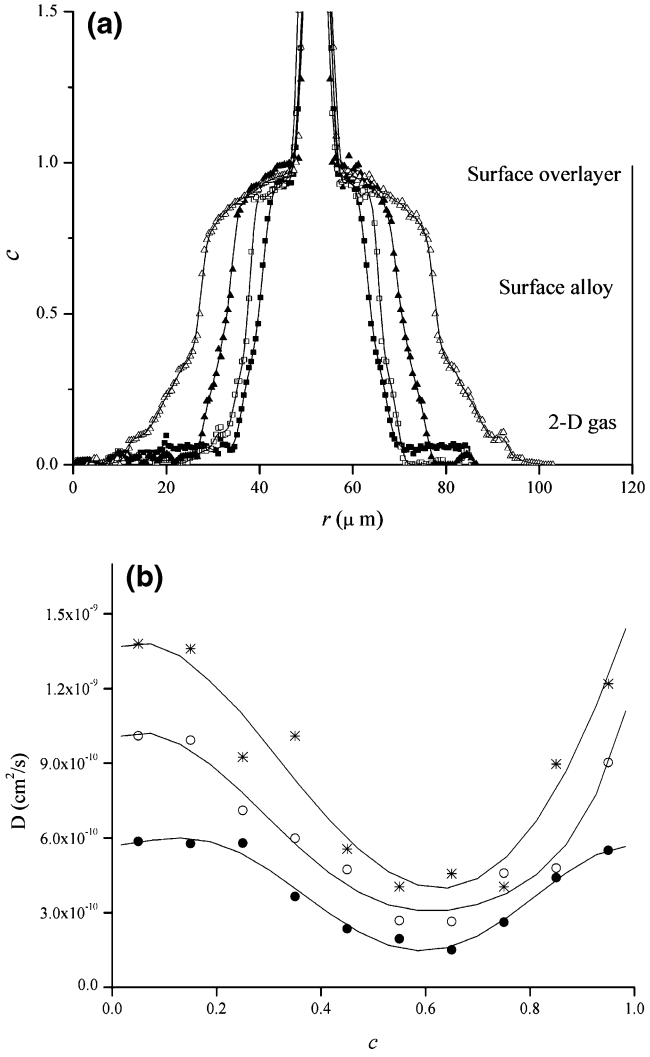

Figure 9. (a) Spreading profiles at 373 K: (■) 15; (□) 30; (▲) 75; and (△) 120 min. (b) Diffusion coefficients of Pb on Cu(111): (●) 353; (○) 363; and (∗) 373 K (see ref 23).

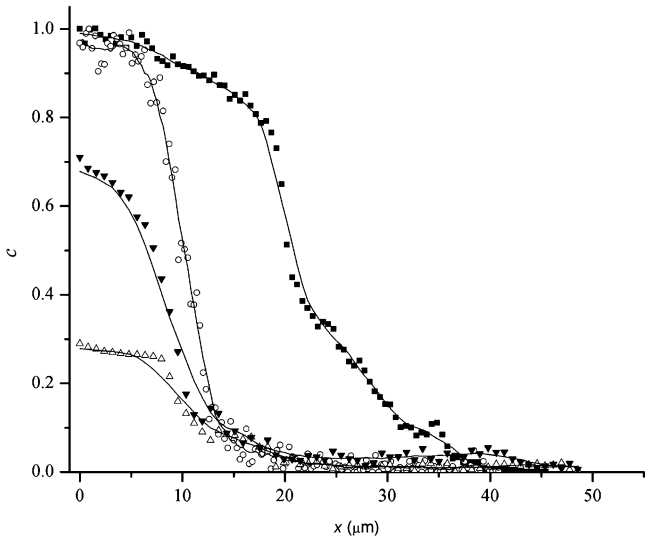

Figure 10. Spreading profiles of pure Pb, pure Bi, and the Pb−Bi alloy on Cu(111) at 373 K: (■) pure Pb, 2 h; (○) pure Bi, 8 h; (△) alloy Pb, 8 h, 30 min; (▼) alloy Bi, 8 h, 30 min.

pure Bi, but detailed analysis[34] shows that Bi in the alloy is moving more slowly than Bi in a pure film. The Pb kinetics are also slower in the presence of Bi than in the

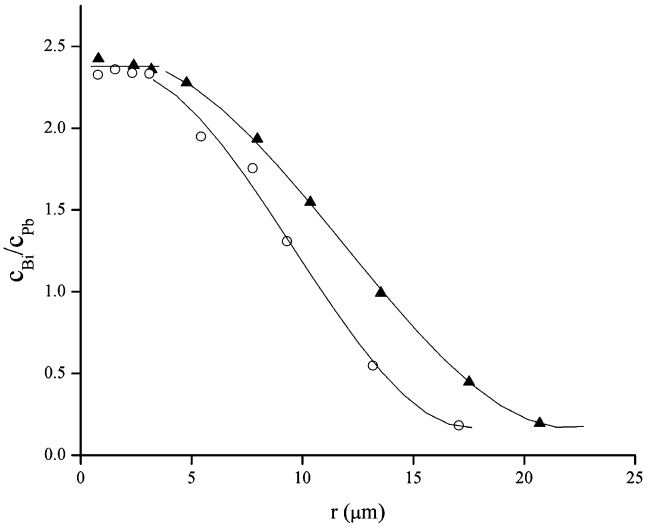

Figure 11. Composition variation in the alloy film as a function of the distance away from the parent drop at 373 K: (▲) 5 h, 30 min; (○) 8 h, 30 min.

pure system. Thus, there appear to be interesting interaction effects in this binary thin film in which the more slowly diffusing Bi tends to slow the spreading of Pb. These effects lead to the low alloy diffusion constant seen in Figure 5. A detailed analysis of these effects will be published elsewhere.

4. Summary

Wetting characteristics and spreading dynamics have been studied by means of AES and SEM for Pb, Bi, and a Pb−Bi alloy on Cu(111), in three regimes, namely, (1) solid drops with a solid film, (2) solid drops with a liquid film, and (3) liquid drops with a liquid film. Special attention has been paid to the precursor films, which spread onto solid substrates, away from the contact line of partially wetting drops.

The equilibrium configurations of all three systems, Pb, Bi, and the Pb−Bi alloy, correspond to pseudopartial wetting, where a near-monolayer thickness precursor film surrounds a drop with a finite contact angle. The macroscopic contact angle near the triple point is found to be insensitive to the temperature or the composition within the ranges studied here.

The spreading profiles and SEM photos obtained in a series of annealing treatments at various temperatures have been used to study the spreading kinetics of precursor films. All experimental results support the view that the spreading mechanism of metallic precursor films is diffusional. Coverage-dependent diffusion coefficients, $D(c)$, can be extracted by means of Fick's second law. The different features of the displayed spreading profiles are not only due to the interaction between the spreading components and the substrate but also due to well-known variations in atomic structure that develop at various surface coverages. In other words, surface reconstruction and surface alloying phenomena must be considered for proper interpretation of precursor film growth mechanisms in metallic systems.

Addition of 11 atom % Bi to Pb slows down the overall kinetics of the spreading. This has its origins in the slower diffusion of Bi compared with Pb and mutual interactions between Pb and Bi in the film. The equilibrium film that coexists with the Pb−Bi drops is highly enriched in Bi, containing as much as 70 atom % Bi at 373 K. The composition of the spreading film varies significantly from the equilibrium value at the contact line to a Pb-rich film at submonolayer coverages.

These studies focus on relatively simple systems, having atomic/molecular architectures with no internal degrees of freedom and no detectable effects due to finite vapor pressure or evaporation. The clear picture of the equilibrium wetting and precursor film growth in these simpler systems elucidate similar properties in more complex systems, for example, rigid molecules with both hydrophobic and hydrophilic moieties such as tricresyl phosphate,[38] polymeric systems with many internal degrees of freedom,[14] surfactant solutions with many degrees of freedom, and potential evaporation and Maragoni flows.[39]

Acknowledgment. The authors wish to acknowledge with thanks support of this research by the National Science Foundation under Grants DMR 9820169 and DMR 9802290.

LA030323J

(38) Shanahan, M.; Houzelle, M.; Carre, A. *Langmuir* **1998**, *14*, 528.
(39) Frank, B.; Garoff, S. *Langmuir* **1995**, *11*, 87.